ELSEVIER

Earth and Planetary Science Letters 138 (1996) 121–135

EPSL

A precursor to the Matuyama/Brunhes transition-field instability as recorded in pelagic sediments

Paul Hartl [a], Lisa Tauxe [a,b,*]

[a] *Scripps Institution of Oceanography, La Jolla, CA 92093, USA*
[b] *Fort Hoofddijk Paleomagnetic Laboratory, Budapestlaan 17, 3584 CD Utrecht, The Netherlands*

Received 30 May 1995; accepted 30 November 1995

Abstract

The period some 20–25 kyr just prior to the most recent generally recognized geomagnetic field polarity transition, the Matuyama-to-Brunhes reversal, appears to be marked by significant geomagnetic variability, manifested as pronounced oscillations in intensity. We compare several previously published paleomagnetic records with new high resolution paleomagnetic data obtained from five pelagic marine sites: North Atlantic DSDP Hole 609B; equatorial Atlantic ODP Hole 665A; and western equatorial Pacific ODP Holes 803B, 804C, and 805B. Using standard rock magnetic normalization for all of the samples, as well as a Thellier/Thellier method on the sediments of Hole 804C, we consistently find a decrease in paleointensity (DIP of [1]) approximately 15 kyr prior to the Matuyama-to-Brunhes transition in the five new records, as well as in the previously published records. Despite sedimentation accumulation rates (SAR) that range from 11 cm/kyr to 1 cm/kyr, these sequences yield paleointensity curves that are broadly similar in form, even at the lowest SARs. The intensity of the pre-reversal low (DIP1) appears to be of the same magnitude as that of the transition itself (DIP2 of [1]). In some of the records, a directional excursion to nearly full normal polarity accompanies DIP1 and remains after alternating field (AF) and/or thermal demagnetization, whereas in other records the directional changes vanish with demagnetization and appear to be caused by overprinting. A viscous remanent magnetization (VRM) contribution to NRM was identified in two of the records and, until removed by AF or thermal demagnetization, was found to blur the 'double-DIP' nature of the paleointensity profiles into an apparent single-DIP, and also resulted in an apparent, but erroneous, 'sawtooth'-like post-transitional sudden increase in paleointensity. After appropriate normalization, the magnitude of the post-transitional recovery was much reduced. The magnetic directions of three of the new records after 'cleaning' and adjusting the stable declinations to either 0 (normal) or 180 (reverse), map to VGP positions lying in the Pacific; the directional variations, however, are far less consistent than the intensity variations. The confirmed global existence of this DIP so closely preceding a major reversal invites questions about its relation to the reversal itself. The apparent normal character of this interval can also present problems for magnetostratigraphical interpretations based on coarse or incomplete sampling by mimicking the Brunhes/Matuyama reversal some 15 kyr earlier in the section than its true location.

Keywords: Brunhes Epoch; Matuyama Epoch; paleomagnetism; rock magnetic normalization; Thellier method; depositional remanent magnetization; reversal

* Corresponding author. E-mail: ltauxe@geof.ruu.nl

SSDI 0012-821X(95)00231-6

1. Introduction

The ~ 780,000 year old Brunhes/Matuyama geomagnetic polarity reversal, being the most recent and often the best preserved reversal, is also one of the most studied in paleomagnetism, serving as a benchmark by which older reversal records are measured (for a review, see [2]). Curiously, however, relatively little attention has been paid to the period just prior to the reversal until recently [1,3], although many records indicate that the geomagnetic field experienced marked fluctuations at that time [4–10]. In this paper we investigate the period from 40 kyr before the Brunhes/Matuyama reversal to 10 kyr afterwards, comparing new high resolution data we have recently obtained from five DSDP and ODP holes with records from seven other pelagic locations. As can be seen from Fig. 1, this suite of twelve sites is widely dispersed over the Earth's surface and also displays a wide range in SARs, from 1 cm/kyr to 11 cm/kyr (Table 1).

2. Methods

Small samples of approximately 1 cm^3 volume were taken at 1–3 cm intervals across the zone of interest from cores from DSDP Leg 94 Hole 609B, ODP Leg 108 Hole 665A and ODP Leg 130 Holes 805B, 804C, and 803B (Table 1). In addition, duplicate samples were collected across the low paleointensity interval (apparent from shipboard records) centered at approximately 15 kyr prior to the Matuyama/Brunhes transition, in order to conduct paired thermal and alternating field (AF) demagnetization studies. The AF demagnetized samples were subsequently used to measure anhysteretic remanent magnetization (ARM), saturation isothermal remanent magnetization (SIRM) and magnetic susceptibility (χ).

All remanence measurements were made with the 2-G Enterprises superconducting cryogenic magnetometer housed in the low-field room of the paleomagnetics laboratory at Scripps Institution of Oceanography in La Jolla, California. All specimens were subjected to stepwise alternating field demagnetization, except for those from Hole 804C and selected duplicate samples from Holes 609B, 803B, and 805B, which were subjected to stepwise thermal demagnetization. Stepwise AF demagnetization was performed using a Schonstedt alternating field demagnetizer and stepwise thermal demagnetization was conducted using a Schonstedt thermal specimen demagnetizer. ARM was imparted with a 0.05 mT bias field and an 85 mT alternating field. SIRM was imparted in an 0.6 T impulse field. Magnetic susceptibility was measured on a Kappa Bridge KLY-2.02 susceptibility bridge.

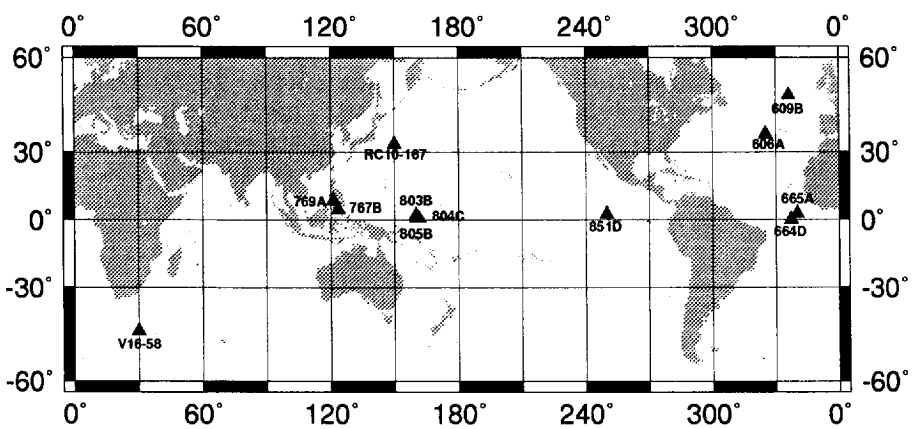

Fig. 1. Site location map for the twelve cores listed in Table 1. New high resolution time series data were collected for this study from DSDP and ODP Holes 609B, 665A, 805B, 804C and 803B. Data from the other seven sites were obtained from pre-existing studies.

Cores from ODP Holes 803B, 804C, 805B and 665A were chosen for this study because: (1) the shipboard magnetic measurements indicated the presence of an apparent short duration normal polarity subchron at approximately 15 kyr before the Brunhes/Matuyama boundary; (2) these cores had previously been only lightly sampled and thus were relatively undisturbed; and (3) previous work on cores from the Ontong–Java Plateau [7,11,12] indicated the probable magnetic carrier to be stable, pseudo-single domain magnetite and thus we felt that nearby ODP holes 804C and 805B would be suitable for paleointensity study [13,14]. DSDP Hole 609B was included in this study out of a desire to extend the excellent Brunhes/Matuyama transition record obtained from Hole 609B by Clement and Kent [15] backward in time some 25 kyr. Hole 609B's high latitude location and high SAR of approximately 7 cm/kyr also serve to broaden the coverage of the database.

SARs were taken for the most part from published estimates using an age of 780,000 yr for the Brunhes/Matuyama boundary [16]. The methods used to arrive at these estimates varied from a simple calculation using only the depth to the B/M boundary (664B, 665A [5]; V16-58) [17], to calculations averaging Brunhes and Matuyama rates based on depths to the B/M and the upper Jaramillo transition (609B, 606A [15]; 767B, 769A, [3]; 803B, 804C, 805B, [18]), to methods using astronomical periodicities in density time-series data (851D) [9].

In order to calculate virtual geomagnetic pole (VGP) positions from these unoriented cores, a zone of stable polarity, either reverse or normal, was identified within each core section. The declinations were adjusted by a constant factor such that the resulting mean declination of the directionally stable zone was either 0 for normal sections or 180 for reverse cases.

Vector end-point diagrams of Brunhes samples from these cores indicate simple demagnetization behavior (Fig. 2a–d). Stable Matuyama specimens exhibit small viscous overprints upon a reverse magnetization (Fig. 2e, 2g and 2h) or apparently single-component reverse behavior (Fig. 2f). Many specimens taken from the low-paleointensity interval some 15 kyr prior to the Brunhes/Matuyama boundary (DIP1) [1,3] exhibit demagnetization paths that indi-

Table 1
Site latitude, longitude, SAR and depth to the Brunhes/Matuyama boundary for the twelve records of this study (locations shown in Fig. 1)

Hole	Lat (N)	Long (E)	SAR (cm/kyr)	B/M depth(m)	reference
804C	1.00	161.4	1.0	6.69	[18], this paper
803B	2.26	160.3	1.0	7.72	[18], this paper
V16-58	-46.00	30.0	1.0/1.4	11.30	[1], this paper
RC10-167	33.40	150.4	2.0	14.70	[28]
805B	1.14	160.32	2.0	12.65	[18], this paper
851D	2.77	249.40	2.0	13.50	[9]
665A	2.95	340.33	2.0	14.72	[5]
606A	37.33	324.50	3.0	19.90	[15]
664D	0.10	336.70	3.6	27.80	[25]
609B	49.86	335.77	7.0	48.82	[15], this paper
767B	4.78	123.50	7.0	48.82	[3]
796A	8.78	121.30	11.0	62.27	[3]

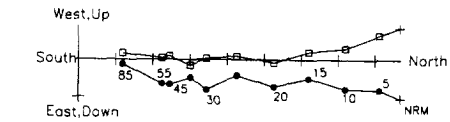

803B-02H-03-32, ticks=1.0e-09 Am²
Brunhes chron, AF demagnetization (a)

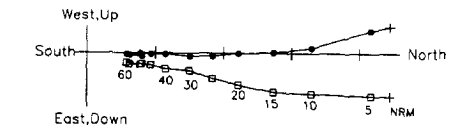

665A-03H-02-51, ticks=5.0e-09 Am²
Brunhes chron, AF demagnetization (b)

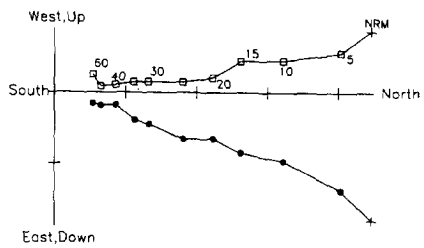

805B-02H-04-138, ticks=1.0e-09 Am²
Brunhes chron, AF demagnetization (c)

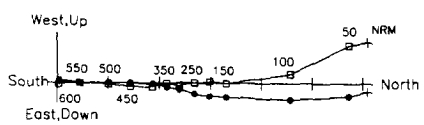

804C-02H-02-25, ticks=5.0e-09 Am²
Brunhes chron, thermal demagnetization (d)

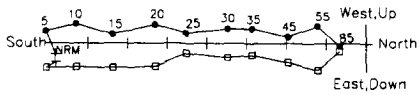

803B-02H-03-80, ticks=1.0e-09 Am²
Matuyama chron, AF demagnetization (e)

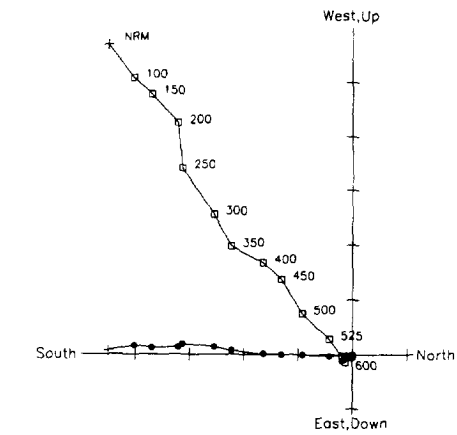

609B-06-02-40,=1.0e-08 Am² (f)
Matuyama chron, thermal demagnetization

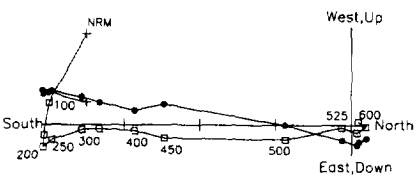

805B-02H-05-53, ticks=1.0e-09 Am²
Matuyama chron, thermal demagnetization (g)

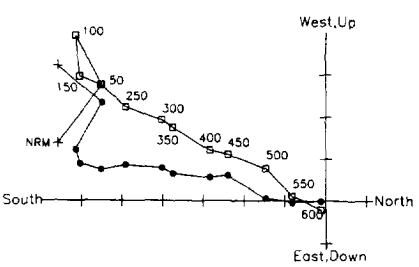

804C-02H-02-64, ticks=5.0e-09 Am²
Matuyama chron, thermal demagnetization (h)

Fig. 2. Orthogonal vector diagrams depicting alternating field (AF) and thermal demagnetization behavior of selected specimens from the four cores sampled for this study. Brunhes normal magnetization is evident in (a)–(d), whereas typical Matuyama reverse behavior can be observed in (e)–(h). Plots (i)–(n) depict demagnetization paths of specimens from within a Matuyama low-intensity zone, which we observe in all cores approximately 15 kyr before the Matuyama-to-Brunhes transition (see text). The complex demagnetization paths of these specimens suggest a 'softer' and subsequent normal overprinting of an original low intensity reverse magnetization. Dots are the projection of the remanence vector at each step onto the horizontal plane and open squares are projections onto the vertical plane.

cate a weak and somewhat erratic Matuyama polarity, with a relatively strong (but soft) viscous overprint (Fig. 2i–k, 2m, 2n). Principle component analyses (PCA) [19] of these samples yield VGP positions that are not fully reverse but, rather, exhibit some 'excursionary' behavior. Others (e.g., Fig. 2l) suggest reasonably stable, fully normal polarity.

Plots of the 'rock magnetic' parameters ARM

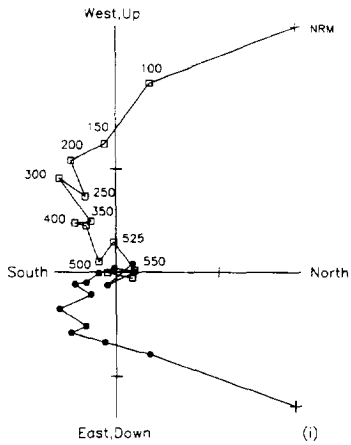

805B-02H-05-26, ticks=5.0e-10 Am²
Brunhes precursor, thermal demagnetization

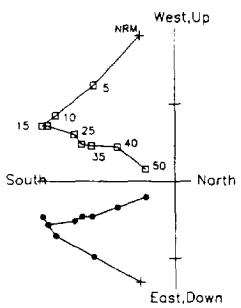

805B-02H-05-21, ticks=5.0e-10 Am²
Brunhes precursor, AF demagnetization

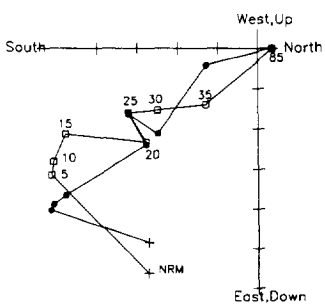

803B-02H-03-58, ticks=2.0e-10 Am²
Brunhes precursor, AF demagnetization (k)

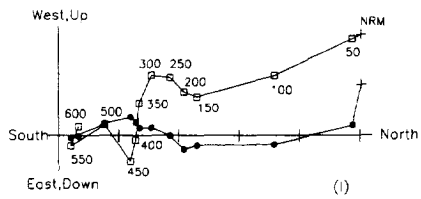

804C-02H-02-49, ticks=5.0e-10 Am²
Brunhes precursor, thermal demagnetization

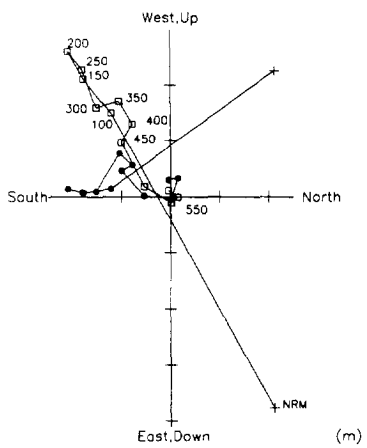

609B-06-02-25, ticks=2.0e-09 Am²
Brunhes precursor, thermal demagnetization

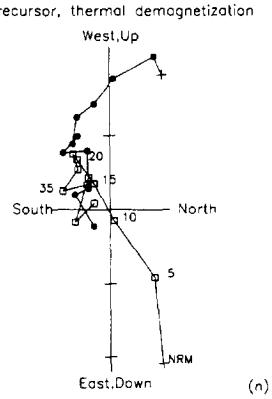

609B-06-02-25, ticks=5.0e-09 Am²
Brunhes precursor, AF demagnetization

Fig. 2 (continued).

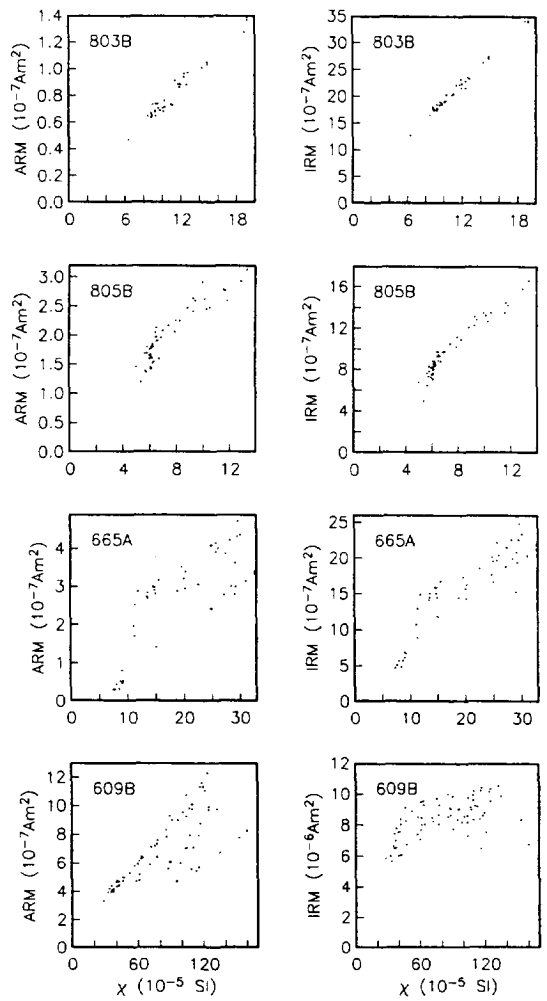

Fig. 3. ARM versus χ and IRM versus χ for the four cores investigated for this study.

versus χ and IRM versus χ for four records are shown in Fig. 3 (Due to the stepwise thermal demagnetization procedure used for Hole 804C specimens, it was not possible to measure ARM and IRM for those specimens). The desired behavior for paleointensity determinations is a linear relation between ARM and χ and IRM and χ [13,14]. 803B and 805B exhibit good behavior by this measure, but 609B and 665A are clearly less than ideal. An assessment of whether this non-ideal behavior seriously compromises paleointensity determinations will become more clear when depth is considered.

For specimens from ODP Hole 804C, we used the Thellier/Thellier [20,21] method and compared these results with a more standard χ-normalized $ChRM_{300}$ (NRM demagnetized at 300°C) paleointensity method. The Thellier/Thellier method is usually employed to estimate absolute paleointensity from igneous rocks containing a natural thermal remanent magnetization (TRM), whereas our samples are sediments that carry a detrital remanent magnetism (DRM) that is far less efficiently acquired and much less well understood than TRM [14]. However, the Thellier/Thellier method, should it prove successful, could allow for a better separation of viscous overprint components from the original DRM [22] and may thereby lead to a more accurate overall picture of the relative paleointensity changes across the B/M boundary. Absolute intensity determinations are not attempted as the relative efficiency of DRM processes is unknown and is very likely to be dependent on sediment types and conditions.

Fig. 4 includes Arai plots [23] from three Hole 804C samples, one each from the Brunhes, the Brunhes precursor (DIP1), and the Matuyama portions of the core (for detailed discussions on Arai plots, see [24]). Assuming that both the NRM and laboratory-produced TRM increase linearly with increasing field strength; that is, $NRM = k_1 B_G$, and $TRM = k_2 B_L$, (where B_G = geomagnetic paleointensity, B_L = laboratory field intensity, and k_1 and k_2 are constants representing the efficiency of DRM and TRM acquisition, respectively), then the change in NRM over the change in TRM in a particular unblocking interval, $\Delta NRM_i/\Delta TRM_i$, should equal $k_1 B_G/k_2 B_L$, or:

$$B_G \alpha \Delta NRM_i/\Delta TRM_i$$

Graphically, this amounts to simply finding the (negative) slope of a best-fit line $(-\Delta y/\Delta x)$ to arrive at a paleointensity estimate for each sample, provided that the slope is sufficiently constant over successive intervals to be determinable. A complicating factor comes from the influence of viscous remanence (VRM), which is acquired at low temperature over time periods not reproducible in the laboratory. If a sample has appreciable VRM, $\Delta NRM_i/\Delta TRM_i$ at lower temperature intervals will be too steep. However, as VRM can reasonably be expected to disappear at higher temperatures, $\Delta NRM_i/\Delta TRM_i$ should remain relatively constant as temperature is

increased. The influence of VRM can be seen in all three of the plots in Fig. 4 in which the slope is greater at lower temperatures, but decreases to a more stable value at higher successive temperatures.

Also represented on these plots, by the L-shaped lines and open triangles, are 'back p-TRM checks' whereby we monitored chemical changes in the magnetic carrier, induced at high temperature by comparing a p-TRM acquired at a particular temperature with a p-TRM acquired later at the same temperature, but after the sample had been subjected to higher-temperature demagnetization (see [24]). No change in the magnetic carrier results in a perfect overplotting of the open triangle over the filled circle of a particular temperature. As can be seen, only a small discrepancy is indicated, and thus little high-temperature chemical alteration of the magnetic carrier occurred as a result of the heating steps.

3. Results

Fig. 5a depicts our high resolution results for ODP Hole 805B, which includes the Brunhes/Matuyama boundary at 12.65 mbsf (meters below seafloor). At an approximate SAR of 2 cm/kyr (Table 1) this 135 cm record covers a period of approximately 50 kyr before and 15 kyr after the transition. We plot both the natural remanent magnetization (NRM) and the remanence left after the specimen was 'cleaned' in a 20 mT alternating magnetic field, which we deduce, from principle component analysis of the vector diagrams of Fig. 2, to be the characteristic remanent magnetization (ChRM). The declination of this equatorial record best marks the reversal at 12.65 mbsf; also apparent is a directional excursion at approximately 12.95 mbsf, or some 15 kyr before the Brunhes/Matuyama boundary. This feature is strongly present in the NRM directions but is somewhat subdued in the ChRM (as can also be observed in Fig. 2i and 2j).

The uppermost plot in Fig. 5a is a record of the remanent intensity (NRM and ChRM) normalized to account for variations in magnetic carrier concentration by three different rock magnetic parameters, ARM, IRM and χ. In order to compare the different estimates of relative intensity, we further normalized these data by the mean of the record — hence all

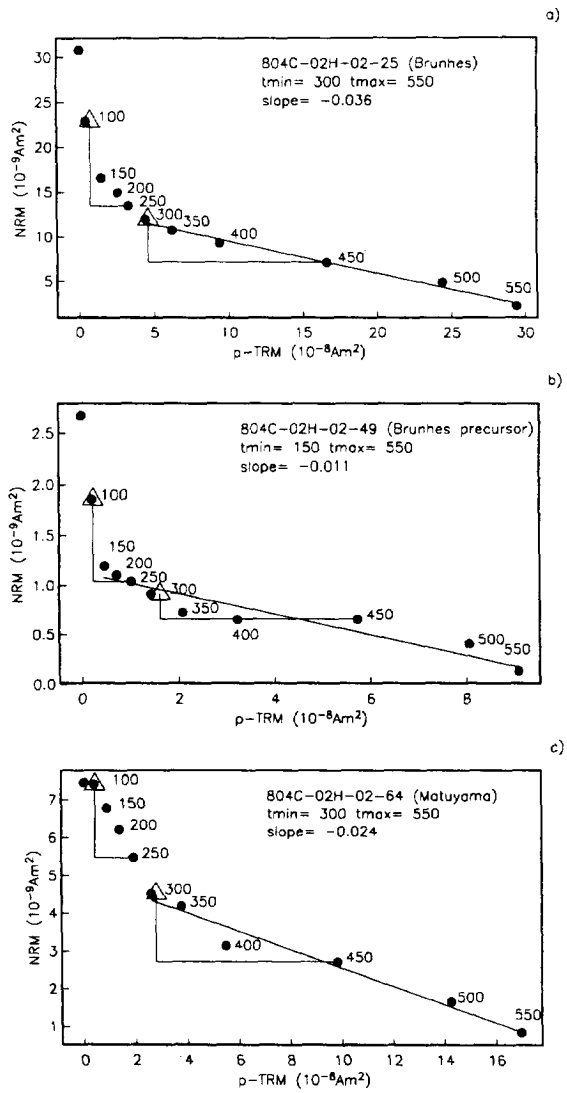

Fig. 4. Arai plots [21] from Hole 804C. The y axis indicates the NRM intensity remaining after successive thermal demagnetization steps, the x axis indicates the intensity of the partial thermal remanent magnetization (p-TRM) gained by subjecting the sample to a 50 mT field at the same temperature. The negative slope of the indicated best-fit line is used to arrive at a paleointensity estimate (see text). Viscous remanence (VRM) produces a slope that is greater at lower temperatures but disappears to produce a more stable value at higher temperatures. L-shaped lines and open triangles represent 'back p-TRM checks', whereby chemical changes in the magnetic carrier produced by the high temperature treatment are monitored by comparing p-TRM acquired at a one temperature with a p-TRM later acquired at the same temperature, but after the sample had been subjected to a higher temperature demagnetization step (see text).

fluctuations are relative to unity. This normalization procedure, if successful, should give identical patterns of relative intensity, regardless of the normalization parameter. Any significant change in rock magnetic ratios indicative of changes in magnetic mineralogy or grain size [13,25] reveal themselves as deviations of one curve with respect to another. Apart from the deviation of the NRM/IRM curve from the ChRM curves, the highly parallel nature of the curves is evidence that the amplitude variations are not controlled by environmental effects. The relative intensity pattern exhibits a prominent low at 12.95 mbsf (DIP1) only after the viscous normal overprint is removed (compare NRM with ChRM

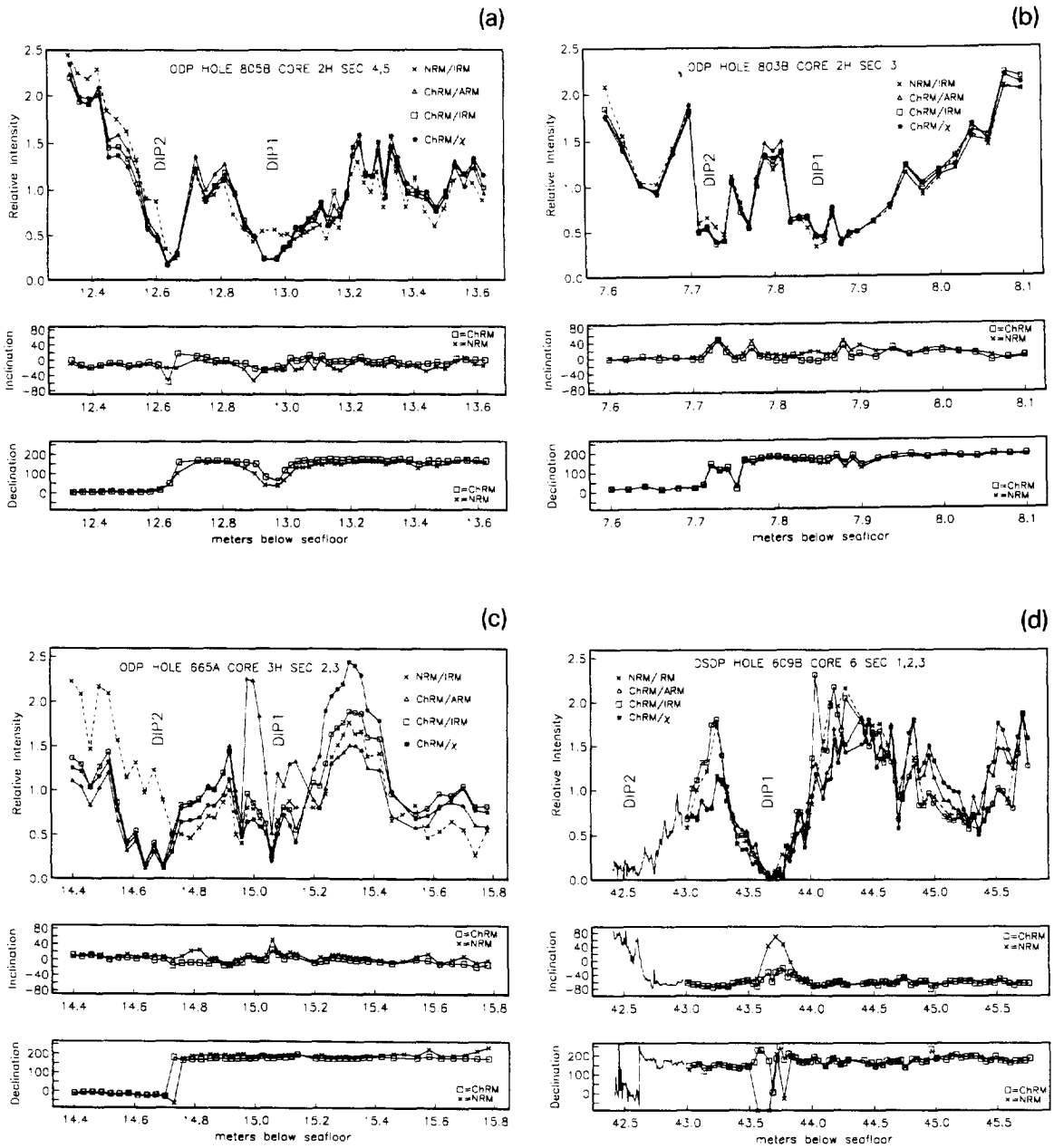

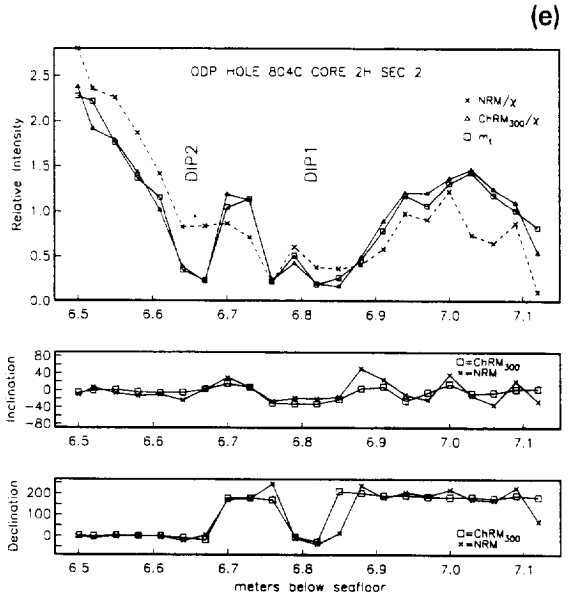

Fig. 5 (continued).

curves). Note that DIP1 at 12.95 mbsf is approximately of the same magnitude as found at the reversal at 12.65 mbsf (DIP2).

Fig. 5b similarly depicts our results for nearby ODP hole 803B in which the Brunhes/Matuyama boundary is most evident in the declination record at 7.72 mbsf. Associated with the reversal are fluctuations in remanent directions and a DIP spanning from 7.71 to 7.78 mbsf. Also apparent is another DIP centered around 7.83–7.94 mbsf which, likewise, is accompanied by directional instabilities. Given an SAR of approximately 1 cm/kyr (Table 1), DIP1 is centered at about 16 kyr before the Brunhes/Matuyama polarity transition. Similar to the 805B results, the three normalized ChRM intensity curves for 803B are quite reproducible, reflecting the rather constant rock magnetics across the interval (see Fig. 3). It is noteworthy that this record, despite its slow SAR of 1 cm/kyr, has clearly preserved a 'double-DIP' paleointensity profile.

Fig. 5c displays our results for equatorial Atlantic ODP Hole 665A. The Brunhes/Matuyama boundary occurs at 14.72 mbsf and is most prominent in the declination record. Some directional instability is observable in both the declination and inclination records centered around 15.05–15.10 mbsf, or about 16 kyr before the Brunhes/Matuyama boundary, based on a sediment accumulation rate of 2 cm/kyr (Table 1), but more interesting is the ChRM intensity record, which exhibits a prominent low at this point and bears resemblance to the intensity records of 805B and 803B. The three curves of normalized ChRM intensity at the top of Fig. 5c are not as consistent as those shown in Fig. 5a and b. ARM and

Fig. 5. (a) Magnetic remanence declination, inclination, intensity and normalized intensity record from equatorial Pacific ODP Hole 805B, with the B/M transition at 12.65 mbsf. Characteristic remanent magnetization (ChRM) was obtained after 20 mT alternating field demagnetization treatment. Normalized intensities are set to a mean of unity and superposed for comparison. The highly parallel trends of the three intensity normalizations indicate nearly constant ratios of ARM/χ, IRM/χ and ARM/IRM and demonstrate the unchanging nature of the magnetic carrier across this interval. The intensity low at 12.95 mbsf precedes the B/M transition intensity low by about 15 kyr (SAR = 2 cm/kyr) and is characterized by equally low magnetizations but only small directional changes. (b) Magnetic record for ODP Hole 803B as for Hole 805B in (a). The B/M boundary is at 7.72 mbsf. The paleointensity low centered at 7.88 mbsf precedes the reversal's intensity low by about 16 kyr (given a SAR of 1 cm/kyr) and is also accompanied by small directional changes, much as for nearby Hole 805B. (c) Magnetic record for equatorial Atlantic Hole 665B, as for Hole 805B in (a). The B/M boundary is at 14.75 mbsf. The paleointensity low at 15.05 mbsf precedes the reversal by 15 kyr (SAR = 2 cm/kyr), much as for the Hole 805B and 803B records. The less parallel nature of the normalizations indicates small changes in rock magnetic properties across the interval. (d) Magnetic record for North Atlantic DSDP Hole 609B. The portion from 42.40 to 43.00 mbsf is data from Clement and Kent [15]. The rest is from this study. The Brunhes/Matuyama boundary is at 42.65 mbsf. The paleointensity low at 43.75 mbsf precedes the reversal by 16 kyr (SAR = 7 cm/kyr), much as for the 805B, 803B, and Site 665A records. The three normalizations of ChRM, although not in very good agreement, all yield a similar broad paleointensity record, and bear strong resemblance to those in (a) and (b). (e) Magnetic record for equatorial Pacific Hole 804C with B/M boundary at 6.69 mbsf. The $ChRM_{300}/\chi$ data were obtained from thermal demagnetization of specimens at 300°C and normalization using χ. The m_t data were obtained from a Thellier/Thellier analysis (see text and above for description). Note the remarkable agreement obtained from the two different methods and the single-DIP character of the NRM signal. Also note that the direction changes associated with DIP1 persist despite thermal demagnetization 'cleaning'. The paleointensity low at 6.85 mbsf precedes the reversal by 16 kyr (SAR = 1 cm/kyr), yielding a 'double-DIP' record similar to those for Holes 805B, 803B, 665A and 609B.

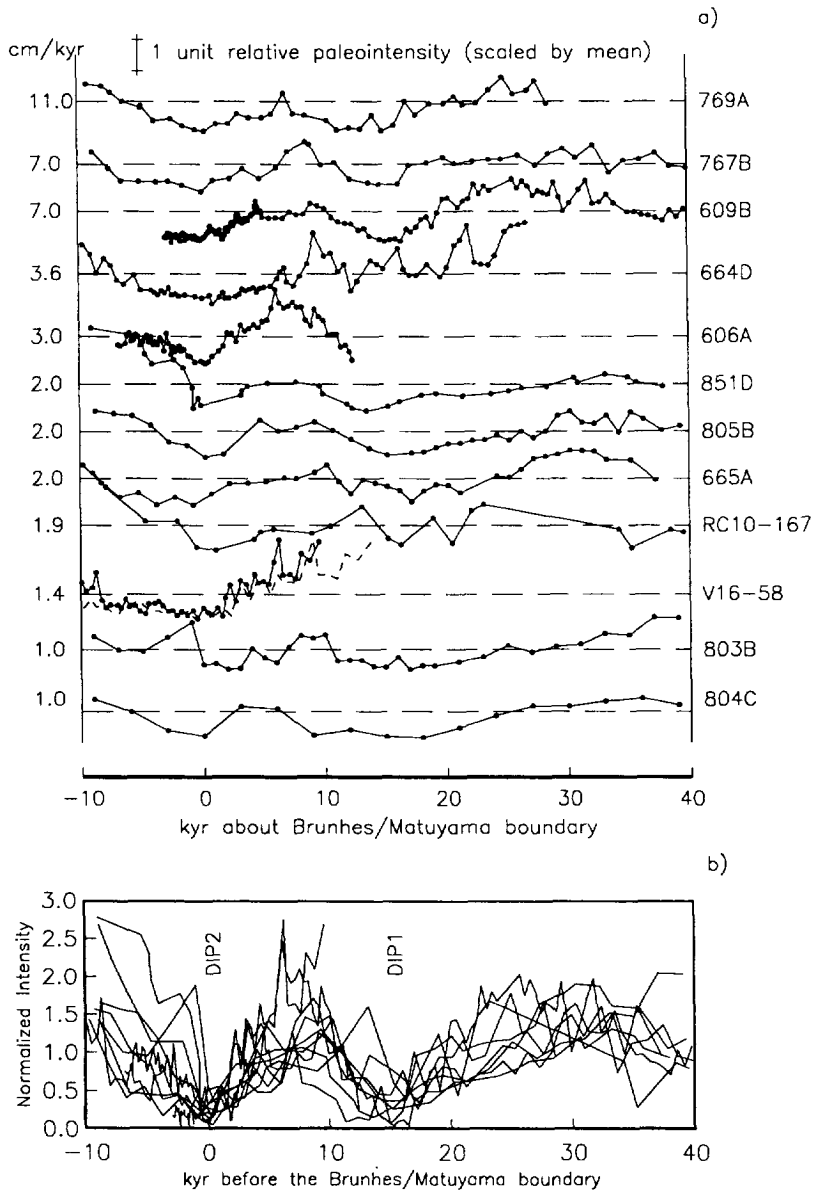

Fig. 6. (a) Paleointensity records from the twelve pelagic cores listed in Table 1 and whose locations are depicted in Fig. 1. All are normalized by either ARM, IRM or χ and are further normalized to their mean across the interval (scale bar at top indicates one unit of normalized intensity) and set to a common time scale based upon SAR estimates (Table 1). Zero time is set at the Brunhes/Matuyama boundary, which is determined from the directional portion of the paleomagnetic data (not shown here). Note that all records indicate an intensity low at the B/M boundary and a similar intensity low $\sim$ 15 kyr before the boundary, as well as showing similar trends in general. Two SARs are depicted for V16-58: the solid line, at a rate of 1.45 cm/kyr (based only on the depth to the B/M boundary); the dashed line at the 1 cm/kyr rate preferred by [1]. (b) A superposition of the twelve separate paleointensity records depicted in (a), dramatically demonstrating the congruent behavior from these twelve widely dispersed sites.

IRM normalizations are very consistent above about 14.95 mbsf, but the record deteriorates below this, particularly in ARM. Instead of a low at this point, the ARM normalized curve exhibits a pronounced high, in direct contrast to the IRM and χ normalizations, both of which yield curves very much like the three nearly parallel normalizations of Holes 805B and 803B. Compared to Holes 805B and 803B, the Hole 665A ChRM/χ paleointensity curve also exhibits a greater high at 15.35 mbsf (approx. 35 kyr before the Brunhes/Matuyama boundary). Other interesting attributes of this record include the way in which DIP2 is masked by viscous overprinting in the NRM record (but is revealed in the ChRM records) and the false steep rise in paleointensity in the NRM record at the B/M transition. Indeed, if AF demagnetization had not been successful in removing the viscous overprint, the record would indicate a single 'DIP' *before but not during* the B/M transition, followed by an overly steep initial increase in post-transition field strength. Unremoved or unremovable viscous overprints could thus account for the initial portion of the 'sawtooth' paleointensity profiles reported for some recent chrons [4,9], as well the apparent single-DIP nature of the B/M in some records [17,26].

Our results for North Atlantic DSDP Hole 609B are shown in Fig. 5d for the core interval 43.00–45.70 mbsf. The data shown for the adjacent interval from 42.40 to 43.00 mbsf, which contains the Brunhes/Matuyama boundary at the 42.60 m level, is from Clement and Kent [15], and was AF demagnetized at 20 mT. Given a rate of sediment accumulation of 7 cm/kyr for Hole 609B (Table 1), the prominent low intensity interval centered at 43.70 mbsf is centered about 16 kyr before the Brunhes/Matuyama transition, much as was found for Holes 805B, 803B and 665A. The inclination record of the undemagnetized NRM indicates a full normal polarity excursion at 43.70 mbsf; whereas, after a treatment of 20 mT AF demagnetization, the remaining inclinations have deviated far less and are of reverse polarity. Thermal demagnetization is equally effective (compare Fig. 2m and n) and we thereby conclude that much of this apparent 'normal' is due to viscous overprinting during the Brunhes. The three normalized intensity curves of Fig. 5d (ChRM/ARM only for the data of Clement and Kent [15]) are more nearly parallel than those for Hole 665A (Fig. 5c) but less so than those of Holes 805B and 803B.

Although some rock magnetic variation is clearly present, the prominent double 'DIP' shape of the paleointensity curve from Hole 609B is quite similar to those of 805B, 803B and 665A.

Fig. 5e depicts our results for Hole 804C in a manner similar to Fig. 5a–d. The only difference here is that Fig. 5e has no ARM or IRM-normalized paleointensity estimate but, instead, substitutes our Thellier/Thellier results (normalized to a unity mean) and directly compares them with a more standard χ-normalized ChRM (after 300°C thermal demagnetization). The results of the two very different methodologies are remarkably similar, and once again indicate a 'double-DIP' paleointensity profile at the B/M boundary. Also interesting is the NRM/χ record, which, much like that of Hole 665A (Fig. 5d), indicates an incorrect single-DIP profile at the B/M boundary, with the DIP and partial recovery occurring well before the directional change; the latter is largely unaffected by the VRM portion of the NRM. Also similar to the NRM record of Hole 665A (Fig. 5d) is the overly steep post-transition rise in apparent paleointensity due again to the VRM contribution to NRM.

4. Discussion

It is clear from Fig. 5a–e that these five cores display a similar record of intensity variations just prior to and during the Brunhes/Matuyama transition, and that the deviations from ideal rock magnetic behavior, while affecting the amplitudes, do not obscure the major trends in paleointensity. The variability between the different methods of normalization gives us some idea of the uncertainty in the relative paleointensity estimates.

We next compare our five new paleointensity records with previously published high resolution paleointensity records from ODP Holes 767B and 769A [3], Hole 851D [9], Hole 664D [27], DSDP Hole 606A [15], core V16-58 [17], and core RC10-167 [28]. In Fig. 6a all twelve paleointensity records are plotted against time about the Brunhes/Matuyama boundary.

The sediment accumulation rates were calculated as outlined previously in the 'methods' section. The exact location of the Brunhes/Matuyama boundary for each case in Fig. 6 was chosen from the directional data (not shown), not from the lowest point of the paleointensity curve. Note that, because the various authors have used different normalization schemes, we have chosen to present all paleointensity data normalized to the mean over the interval. Finally, in Fig. 6b we superpose all twelve records to demonstrate the consistent results obtained from these combined data.

All twelve cores depicted in Fig. 6 yield a paleointensity record that is similar, in spite of the great diversity of site locations and SARs (see Table 1). (Note that we plot the V16-58 record twice in Fig. 6a, the solid line reflects an SAR calculation based on the total depth to the B/M boundary, the dashed line results from a ^{10}Be-based interpretation of Kent and Schneider [1].) Moreover, even in cases of low SARs such as 803B and 804C (~ 1 cm/kyr) and RC10-167, 851D, 665A and 805B (~ 2 cm/kyr), we note that the record is a reasonable facsimile of those from much higher SARs, such as 609A, 767B and 769A. As our analyses of the Holes 665A and 804C results indicate, the apparent smearing of the double-DIP into a single DIP, often attributed to smoothing in the remanence lock-in process [1], is more likely to be due to unremoved VRM components of the NRM.

Directional records from the 'Brunhes precursor' in four of the five holes we sampled are shown in Fig. 7 in terms of VGPs (derived from PCA). VGPs from Holes 609B (SAR = 7 cm/kyr) and 805B (SAR = 2 cm/kyr) indicate brief excursionary behavior for the Brunhes precursor, whereas VGP positions from Hole 803B (SAR = 1 cm/kyr), show a much smaller deflection from full reverse pole position. In direct contrast, the record from 804C depicts two VGPs of almost normal polarity during the Brunhes precursor, even though Sites 803B and 804C are in close proximity to one another and share the same SAR. Hole 665A VGPs (not shown) indicate almost no deflection across the Brunhes precursor. Comparison with the directional records from ODP Holes 767B and 769A also appear to exhibit conflicting results. While 769A shows excursionary behavior, 767B does not [3], despite the fact that the SAR

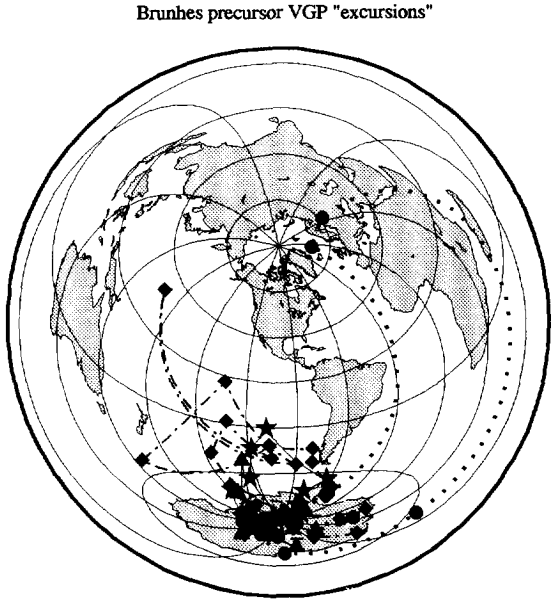

Fig. 7. Virtual geomagnetic pole (VGP) positions obtained from principal component analysis (PCA) of specimens from Holes 609B (◆/dashed line), 803B (▲), 805B (★), and 804C (●/dotted line) across the 'Brunhes precursor' low intensity zone 15 kyr before the Matuyama-to-Brunhes transition. Hole 665A shows even less VGP deviation than 803B, essentially clustering near the South Pole.

of these two cores are the highest available (Table 1). Thus, while the records exhibit good agreement in terms of relative intensity variations and directions across the entire transitional interval, the directional records from samples within the actual DIP intervals from different sites appear to be less reliable. The variability in the directional record may be the work of unremoved overprints, or perhaps the directional changes occurred so rapidly that many records could not track them. However, this latter hypothesis does not square with the fact that 767B, with an SAR of 7 cm/kyr, is nearly devoid of excursionary directions in DIP1 [3]. Furthermore, the equally high SAR 609B record may be instructive in this regard, in that DIP1 NRM normal directions progressively disappear at higher demagnetization steps (both thermal and AF), indicating that these directions arise from

normal overprinting and not from an authentic and primary recording of the DIP1 field directions (see Fig. 5d). We believe that these observations can be generalized to indicate that, in those instances where a DIP1 normal is present in the ChRM as well as the NRM record, such normal directions are simply due to unremoved or unremovable overprinting. We hypothesize that the lack of coherency in DIP1 directions among otherwise high quality and concordant records from neighboring sites, such as ODP 767B and 769A, and the three Ontong–Java Plateau ODP locations, 803B, 804C and 805B, is a result of the very low geomagnetic field strength during DIP1, which left the sediments open to severe VRM overprinting. Small local differences in remanence acquisition conditions within the sediments as the field soon thereafter reversed itself would result in highly variable overprinting from site to site. If, on the other hand, these directions are in fact primary, it is interesting to note the similarity between VGP paths observed in the North Atlantic (609B) with those recorded in the western equatorial Pacific (805B) and the fact that these paths do not coincide with the Americas or Australian tracks proposed by Clement [29].

The anomalously low field intensity and the close temporal proximity of the pre-transition low to the actual Brunhes/Matuyama transition are curious aspects of these records and invite questions as to the exact nature of this feature. Was it part of the reversal itself or an unrelated event that just happened to be followed by a reversal? If field reversals occur when field strength reaches some critically low value, why did the field not reverse and recover strength 15 kyr earlier than it did? These data seem to say that a reversal is made possible when the field strength reaches a certain critically low value, but that the instability can recover by rebuilding to either polarity state, an observation in accordance with calculations [30] based on early geodynamic modeling [31,32]. The first breakdown recovered the earlier condition of reverse polarity and relatively low ambient field strength and was followed shortly thereafter by a second breakdown that recovered to the opposite polarity, but this time to a much greater ambient field strength. Both breakdowns were perhaps made possible because the ambient field strength had deteriorated to such a low value that negative fluctuations about this value brought the field to a critical threshold state, at which point the field could recover to either polarity. Seen in this light, one could say that the two events are related by the low ambient value, but otherwise are distinctly separate.

Another point that should be noted is that this Brunhes precursor often appears in paleomagnetic records as a normal polarity zone, as in our 609B NRM and 804C ChRM record, as well as that of 769B [3]. In the case of cores that are poorly, coarsely or incompletely sampled, perhaps due to breaks in the record, disturbances, or sampling restrictions, it could be easy to mistake this feature for the actual Brunhes/Matuyama boundary. Although an error of 15 kyr would be inconsequential in most cases, there are cases in which such an error could be crucial, such as in investigations into magnetic lock-in depth and the exact calibration of the marine oxygen isotope stages to the paleomagnetic reversal record.

5. Conclusions

1. The similarity and synchroneity of the paleointensity records obtained from twelve globally dispersed sites argues strongly for their accuracy in depicting a time series of the geomagnetic paleointensity prior to the Brunhes/Matuyama boundary. This 'double-DIP' record is typified by two intensity lows separated in time by approximately 15 kyr. The first of these low intensity intervals is not associated with a distinctly identifiable polarity reversal, although some of the records indicate a geomagnetic excursion. The second low is accompanied by the long-term polarity reversal that defines the Matuyama-to-Brunhes transition.
2. The 'double-DIP' paleointensity trend consisting of two paleointensity lows separated by approximately 15 kyr is readily observable in all twelve records despite a wide range in SARs. This observation does not support the conclusion of Kent and Schneider [1] that the double-DIP will be smoothed to a single DIP in cores where the SAR is 1 cm/kyr or less.
3. The contributions of unremoved or unremovable VRM to the NRM may mask the true double-DIP

character of the Matuyama-to-Brunhes reversal in some cores and may very well mask the true nature of other transitions as well. Furthermore, comparison of the ChRM and NRM profiles of Holes 665A and 804C support the contention of [33] that a strong VRM contribution to NRM can also contribute to an apparent 'sawtooth' paleointensity profile, which has been reported for recent chrons [4,9].

4. The fact that DIP1 and DIP2 are preserved as discrete phenomena even in low SAR cores suggests that the magnetic lock-in depth is not as deep as often supposed (e.g., some 16 cm half-depth [1]), but much shallower, perhaps some 3–4 cm, as suggested by [34].

Acknowledgements

The authors would like to thank Steve DiDonna at Scripps and Paula Weiss at the ODP East Coast Repository for technical assistance. This work was supported by NSF grants OCE 89-17252 and OCE92-17966. Funds for paleomagnetic equipment at Scripps were provided by the W.M. Keck Foundation. L. Tauxe gratefully acknowledges partial support from the University of Utrecht. *[MK]*

References

[1] D.V. Kent and D.A. Schneider, Correlation of paleointensity records in the Brunhes/Matuyama polarity transition interval, Earth Planet. Sci. Lett. 129, 135–144, 1995.

[2] B.M. Clement and C. Constable, Polarity transitions, excursions and paleosecular variation of the Earth's magnetic field, Rev. Geophys. Suppl. April, 433–442, 1991.

[3] D.A. Schneider, D.V. Kent and G.A. Mello, A detailed chronology of the Australasian impact event, the Brunhes–Matuyama geomagnetic polarity reversal, and global climate change, Earth Planet. Sci. Lett. 111, 395–405, 1992.

[4] J.-P. Valet, L. Meynadier, F.C. Bassinot and F. Garnier, Relative paleointensity across the last geomagnetic reversal from sediments of the Atlantic, Indian and Pacific Oceans, Geophys. Res. Lett. 21, 485–488, 1994.

[5] L. Tauxe, J.-P. Valet and J. Bloemendal, The magnetostratigraphy of Leg 108 APC cores, Proc. Ocean Drill. Prog. B 108, 865–880, 1989.

[6] L. Tauxe, A.D. Dieno, A.K. Behrensmeyer and R. Potts, Pinning down the Brunhes/Matuyama and upper Jaramillo boundaries: a reconciliation of orbital and isotopic time scales, Earth Planet. Sci. Lett. 109, 561–572, 1992.

[7] Y. Gallet, J. Gee, L. Tauxe and J.A. Tarduno, Paleomagnetic analyses of short normal polarity magnetic anomalies in the Matuyama Chron, Proc. Ocean Drill. Prog. Sci. Res. 130, 547–559, 1993.

[8] D.H. Sun, J. Shaw, Z.S. An and T. Rolph, Matuyama/Brunhes (M/B) transition recorded in Chinese loess, J. Geomagn. Geoelectr. 45, 319–330, 1993.

[9] J.-P. Valet and L. Meynadier, Geomagnetic field intensity and reversals during the past four million years, Nature 366, 234–238, 1993.

[10] R.X. Zhu, Z.L. Ding, H.N. Wu, B.C. Huang, et al., Details of a geomagnetic polarity transition recorded in Chinese loess, J. Geomagn. Geoelectr. 45, 289–299, 1993.

[11] L. Tauxe and G. Wu, Normalized remanence in sediments of the Western Equatorial Pacific, relative paleointensity of the geomagnetic field?, J. Geophys. Res. 95, 12,337–12,350, 1990.

[12] L. Tauxe and N.J. Shackleton, Relative palaeointensity records from the Ontong–Java Plateau, Geophys. J. Int. 117, 769–782, 1994.

[13] J.W. King, S.K. Banerjee and J. Marvin, A new rock magnetic approach to selecting sediments for geomagnetic paleointensity studies: application to paleointensity for the last 4000 years, J. Geophys. Res. 88, 5911–5921, 1983.

[14] L. Tauxe, Sedimentary records of relative paleointensity of the geomagnetic field: theory and practice, Rev. Geophys. 31, 319–354, 1993.

[15] B.M. Clement and D.V. Kent, Geomagnetic polarity transition records from five hydraulic piston core sites in the North Atlantic, Init. Rep. DSDP 94, 831–852, 1986.

[16] N.J. Shackleton, A. Berger and W.R. Peltier, An alternative astronomical calibration of the lower Pleistocene time scale based on ODP Site 677, Trans. R. Soc. Edinburgh Earth Sci. 81, 251–261, 1990.

[17] B.M. Clement and D.V. Kent, A southern hemisphere record of the Matuyama–Brunhes polarity reversal, Geophys. Res. Lett. 18, 81–84, 1991.

[18] L.W. Kroenke, W.H. Berger, T.R. Janacek, et al., Sites 803, 804, and 805, Proc. Ocean Drill. Prog. Init. Rep. 130, 101–290, 1991.

[19] J.K. Kirschvink, The least-squares line and plane and the analysis of paleomagnetic data. Geophys. J. R. Astron. Soc. 62, 699–718, 1980.

[20] E. Thellier and O. Thellier, Sur l'intensité du champ magnétique terreste dans la passé historique et géologique, Ann. Geophys. 15, 285–378, 1959.

[21] T. Pick and L. Tauxe, Holocene paleointensities: Thellier experiments on submarine basaltic glass from the East Pacific Rise, J. Geophys. Res. 98, 17,949–17,964, 1993.

[22] L. Tauxe, T. Pick and Y.S. Kok, Relative paleointensity in sediments: a pseudo-Thellier approach, Geophys. Res. Lett., in press.

[23] T. Nagata, Y. Arai and K. Momose, Secular variation of the geomagnetic total force during the last 5,000 years, J. Geophys. Res. 68, 5277–5281, 1963.

[24] R.S. Coe, S. Grommé and E.A. Maniken, Geomagnetic paleointensities from radiocarbon-dated lava flows on Hawaii and the question of the Pacific nondipole low, J. Geophys. Res. 83, 1740–1756, 1978.

[25] S.K. Banerjee, J.W. King and J. Marvin, A rapid method for magnetic granulometry with applications to environmental studies, Geophys. Res. Lett. 8, 333–336, 1981.

[26] J.-P. Valet, L. Tauxe and D.R. Clark, The Matuyama–Brunhes transition recorded from Lake Tecopa sediments (California), Earth Planet. Sci. Lett. 87, 463–472, 1988.

[27] J.-P. Valet, L. Tauxe and J. Bloemendal, The Matuyama–Brunhes geomagnetic reversal from two deep-sea cores of the eastern equatorial Atlantic, Proc. ODP, Sci. Res. 108, 441–447, 1989.

[28] D.V. Kent and N.D. Opdyke, Paleomagnetic field intensity variation recorded in a Brunhes epoch deep-sea sediment core, Nature 266, 156–159, 1977.

[29] B.M. Clement, Geographical distribution of transitional VGPs: evidence for non-zonal equatorial symmetry during the Matuyama–Brunhes geomagnetic reversal, Earth Planet. Sci. Lett. 104, 48–58, 1991.

[30] Y. Honkura and M. Matsushima, Fluctuations of the nondipole magnetic field and its implication for the process of geomagnetic polarity reversal in the Cox model, J. Geophys. Res. 93, 11,631–11,642, 1988.

[31] A. Cox, R.R. Doell and G.B. Dalrymple, Reversals of the Earth's magnetic field, Science 144, 1537–1543, 1964.

[32] A. Cox, Geomagnetic reversals, Science 163, 237–245, 1969.

[33] Y.S. Kok and L. Tauxe, Saw-toothed pattern of relative paleointensity records and cumulative viscous remanence, Earth Planet. Sci Lett., in press.

[34] C.G. Constable and L. Tauxe, Palaeointensity in the pelagic realm: marine sediment data compared with archaeomagnetic and lake sediment records, Geophys. J. R. Astron. Soc. 90, 43–59, 1987.